POTENTIAL USE OF MULTISPECTRAL AIRBORNE LIDAR DATA IN LAND COVER CLASSIFICATION

Salem Morsy, Ahmed Shaker, and Ahmed El-Rabbany
Department of Civil Engineering, Ryerson University, 350 Victoria St, Toronto, ON M5B 2K3, Canada
Emails: (salem.morsy, ahmed.shaker, and rabbany)@ryerson.ca

KEYWORDS: DSM, Intensity, Maximum Likelihood Classifier, Radiometric Correction

ABSTRACT: Multispectral LiDAR systems either in the form of separate multi-sensor or true multispectral sensors are currently emerging in the market. The multispectral LiDAR sensors operate at different wavelengths that allow recording a diversity of spectral reflectance from land features. This capability improves and extends the applications of LiDAR data. In this context, an improvement of land cover classification is presented from multispectral airborne LiDAR data acquired by the first commercial multispectral airborne LiDAR sensor, the Optech Titan. The sensor operates at three wavelengths; mid-infrared (MIR): 1550 nm, near-infrared (NIR): 1064 nm, and green: 532 nm. In this paper, three intensity images were first created from the collected point clouds at each wavelength, as well as the digital surface model (DSM). A maximum likelihood classifier was then applied to each intensity image separately, combined three-intensity images, and combined three-intensity images with DSM. An urban area, covering Oshawa, Ontario, Canada, was tested to classify the terrain into six classes namely; buildings, trees, roads, grass, soil, and wetland. The classification results were validated using 200 randomly selected reference points. The classification results showed that using single intensity image from wavelengths 1550 nm, 1064 nm, or 532 nm leads to overall classification accuracies of 34.0%, 48.5%, and 41.5%, respectively. The overall classification accuracy was improved to 65.5% using the combined three-intensity images. Moreover, the overall classification accuracy was increased to 72.5% by incorporating the height LiDAR data (i.e., DSM image). In further investigation, a radiometric correction model has been applied to the intensity data to improve the classification accuracy. The overall classification accuracy was improved to 69.0% from the combined three-intensity images and 78.0% by adding the DSM. The results achieved are promising and indicating that the use of multispectral LiDAR data can improve the land cover classification accuracies.

1. INTRODUCTION

Light Detection and Ranging (LiDAR) systems usually operate at near-infrared wavelength (1064 nm), and they acquire range data from the sensor to the Earth surface. In addition, the LiDAR systems record the strength of the backscattered energy reflected from the Earth surface either in the form of discrete intensity values or as full waveform. Currently, multispectral LiDAR sensors are emerging in the market. These sensors acquire multispectral data at different wavelengths. This allows new applications from LiDAR data, in particular using LiDAR data for land cover classification (Yan et al., 2015) and retrieval of biophysical and biochemical vegetation parameters (Wallace et al., 2012). Recently, many experiments have been conducted using laboratory-based multispectral LiDAR systems at wavelengths of 531, 550, 660, and 780 nm (Woodhouse et al., 2011), or 556, 670, 700, and 780 nm (Wei et al., 2012; Shi et al., 2015) for vegetation applications. Other studies have been conducted using multispectral LiDAR data collected by Terrestrial Laser Scanning (TLS) platforms for measuring the three-dimensional structure of forest canopies by two lasers with wavelengths of 1063 nm and 1545 nm (Danson et al., 2014) and discriminating leaves from woody material in forestry area from data collected at two wavelengths of 1064 nm and 1548 nm (Douglas et al., 2015). Few attempts have been conducted using different airborne LiDAR systems by combining different flight missions of the same study area (Briese et al., 2012; Wang et al., 2014). However, it was difficult to use the intensity data came from different missions because those flight missions were conducted at different time.

Teledyne Optech, one of the world leading LiDAR sensor developers and manufacturers, has developed the first commercial multispectral airborne LiDAR sensor, named “Optech Titan”. Optech Titan offers the possibility of multispectral active imaging of the environment at day and night, and thus facilitates new applications and information extraction capabilities for LiDAR. Optech Titan’s standard configuration includes three active laser beams operating at wavelengths of 1550 nm, 1064 nm, and 532 nm (Titan Brochure and Specifications, 2015). That allows capturing discrete and full-waveform data at three independent channels. By combining the multispectral LiDAR data collected by the three different wavelengths, a higher reliability and accuracy of information retrieval can be achieved comparing to the single-wavelength LiDAR systems. Few studies have been conducted for analysing the multispectral LiDAR data collected by the Optech Titan. Geometrical classification procedures were used to classify the LiDAR data. In addition, spectral patterns for different classes were explored and showed that the intensity values could be potentially used in land cover classification (Wichmann et al., 2015). Three spectral indices have been derived from the intensity values of the three channels, and tested for land cover classification and land-water discrimination (Morsy et al., 2016).

This paper aims to investigate the use of the multispectral LiDAR data, collected by the Optech Titan sensor, for land cover classification and explore the effect of applying a radiometric correction model to the intensity data on the classification accuracies. Section 1 of the paper introduces the research problem and motivation. Section 2 discusses the work methodology followed by section 3 describes the study area and dataset. The results and discussions are illustrated in section 4 with conclusions presented in Section 5.

2. METHODOLOGY

The workflow of this research work is shown in Figure 1. The research follows the following steps: a) generating 1m resolution raster intensity images from LiDAR point clouds of the three channels and the DSM, b) training signatures are identified for different classes, c) the maximum likelihood classifier is applied to each intensity image separately, to the combined three-intensity images, and finally to the combined three-intensity images with DSM, and d) 200 checkpoints is randomly selected to assess the overall accuracy.

In further investigation, radiometric correction model has been applied to the intensity data to improve the classification accuracy (Yan et al., 2012). In this context, a radiometric correction approach based on radar range equation is used to remove the system and atmospheric attenuation that affects the recorded intensity data (Yan and Shaker, 2014). Equations (1) and (2) provide the radar range equation, which is used to convert the LiDAR intensity data (P_r) into the spectral reflectance of the ground feature (ρ). The same classification process is then repeated after applying the radiometric correction to the study area.

$$P_r = \frac{P_t D_r^2}{4\pi R^4 \beta_t} \eta_{sys} \eta_{atm} \sigma \quad (1)$$

$$\sigma = 4\pi\rho A cos\theta \quad (2)$$

Where P_t is the transmitted laser power, D_r is the aperture diameter, R is the range, β_t is the laser beam width, η_{sys} is the system factor, η_{atm} is the atmospheric attenuation, σ is the target cross section, A is the projected target area, and θ is the reflection angle.

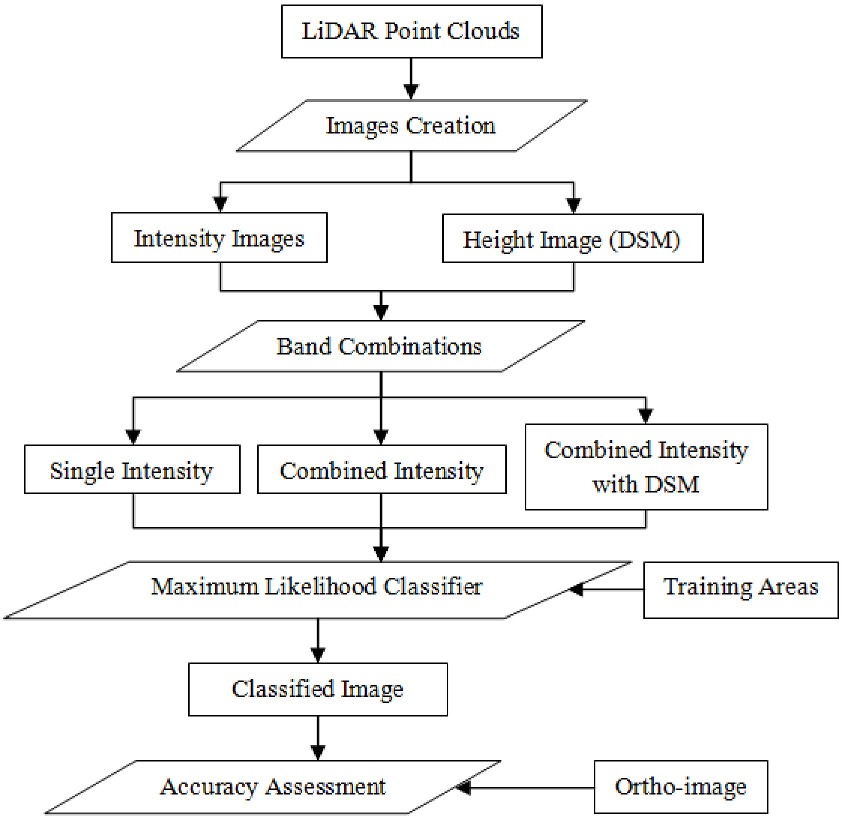

Figure 1. The research workflow

3. STUDY AREA AND DATASET

The study area covers 550m x 380m, and it is located in Oshawa, Ontario, Canada, containing six feature classes: buildings, trees, roads, grass, bare-soil, and wetland. An aerial image of the study area from Google Earth© is shown in Figure 2.

Figure 2. Aerial image of the study area from Google Earth©

The Optech Titan sensor collected 3D point clouds from flying height ~1000m with scanning angle of ±20°. The data is acquired and stored in LAS format with multiple returns (up to 4 returns) for each channel. The LAS data file contains xyz coordinates, intensity values, return number, total number of returns, scan angle, and GPS time. In addition, the trajectory data file, which contains time-tagged xyz coordinates of the sensor location, is provided for radiometric calibration of the intensity data. Figure 3 shows the LiDAR intensity raster images generated from the intensity data of the three individual channels (wavelengths) and the DSM raster image created from the elevation data. The three intensity images from the three channels are combined together and with DSM (Figure 4).

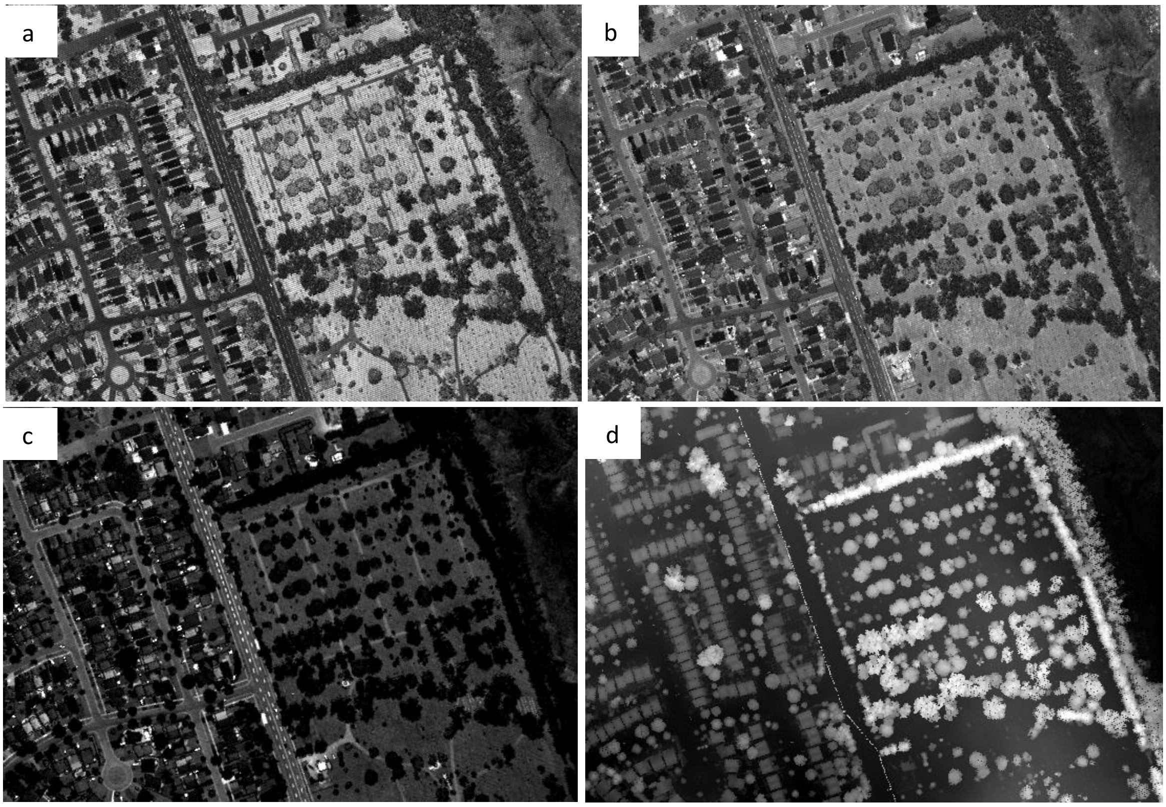

Figure 3. LiDAR images of the study area: a) intensity from 1550 nm, b) intensity from 1064 nm, c) intensity from 532 nm, and d) DSM.

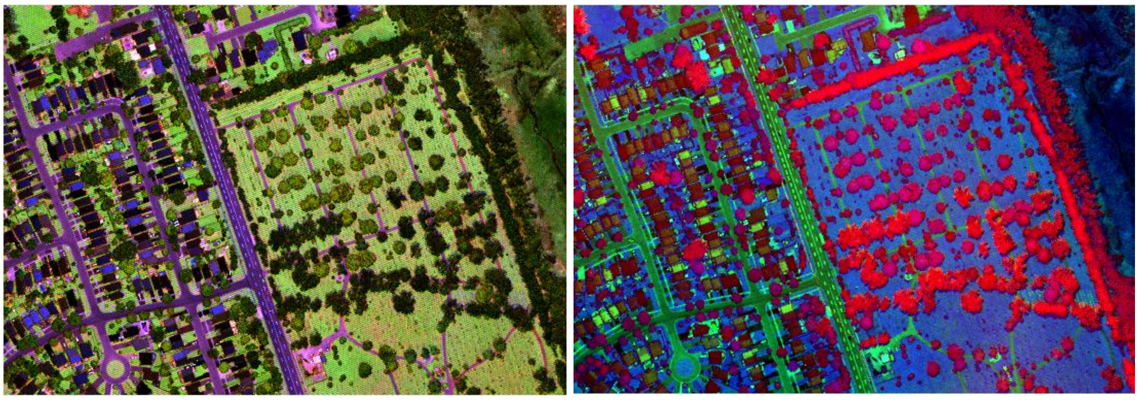

Figure 4. Left: combined three-intensity images (visualized as: 1550 nm in red, 1064 nm in green and 532 nm in blue), and right: combined three-intensity images with DSM (visualized as: DSM in red, 532 nm in green and 1064 nm in blue)

4. RESULTS AND DISCUSSIONS

The classification results from combined intensity images and three-intensity images with DSM are shown in Figure 5. The classification of intensity data from individual channels leads to overall accuracy of 34.0%, 48.5%, and 41.5% from wavelengths of 1550 nm, 1604 nm, and 532 nm, respectively. The overall accuracy is improved to 65.5% and 72.5% when using the combined three-intensity images and incorporating a DSM generated from the elevation data with the combined three-intensity images, respectively. The classification results have proven the benefit of using multispectral data rather than single intensity data, where an improvement of 17.0% is achieved.

Figure 5. Classified images, from combined three-intensity images (left) and combined three-intensity images with DSM (right).

Table 1 and Table 2 provide the confusion matrices of using the combined three raw intensity images without and with DSM, respectively. The results show that the use of LiDAR height data (e.g., DSM) has improved the overall accuracy by 7.0%. That is clear in Figure 5, where some tree pixels are misclassified as wetland class, but they are correctly classified when DSM is considered. Although the combination of intensity data with DSM has achieved good accuracies, some grass pixels are misclassified as soil class at the south-west part of the study area.

Table 1. Confusion matrix of the combined three raw intensity images

Classified points	Reference points							Total	User's
	U	Buildings	Trees	Roads	Grass	Soil	Wetland	row	Acc. (%)
U	0	0	0	0	1	0	0	1	
Buildings	0	14	1	5	1	0	0	21	66.67
Trees	0	8	29	2	5	8	0	52	55.77
Roads	0	1	2	12	2	1	0	18	66.67
Grass	0	0	3	1	60	3	0	67	89.55
Soil	0	5	2	3	3	12	0	25	48.00
Wetland	0	0	10	0	2	0	4	16	25.00
Total column	0	28	47	23	74	24	4	200	
Producer's Acc. (%)		50.00	61.70	52.17	81.08	50.00	100.00		

Overall accuracy: 65.50%, overall Kappa statistic: 0.554

Table 2. Confusion matrix of the combined three raw intensity images with DSM

Classified points	**Reference points**							**Total**	**User's**
	U	**Buildings**	**Trees**	**Roads**	**Grass**	**Soil**	**Wetland**	**row**	**Acc. (%)**
U	0	0	0	0	1	0	0	1	
Buildings	0	19	0	6	1	2	0	28	67.86
Trees	0	6	43	0	10	3	4	62	69.35
Roads	0	1	1	13	2	3	0	20	65.00
Grass	0	0	1	1	55	3	0	60	91.67
Soil	0	2	2	3	5	13	2	27	48.15
Wetland	0	0	0	0	0	0	2	2	100.00
Total column	0	28	47	23	74	24	4	200	
Producer's Acc. (%)		67.86	91.49	56.52	74.32	54.17	50.00		

Overall accuracy: 72.50%, overall Kappa statistic: 0.640

A radiometric correction approach is used to correct the intensity values collected from the three different channels. Figure 6 shows the classification results from combined three-intensity images and combined three-intensity images with DSM after the radiometric correction approach is applied. The classification results after radiometric correction of the intensity data leads to overall accuracy from individual channels of 38.0%, 46.0%, and 52.5% from wavelengths 1550 nm, 1604 nm, and 532 nm, respectively. The overall accuracy of using the combined three-intensity images is improved to 69.0%. The classification results further increased to 78.0% when the combined three-intensity images are used with the DSM.

Generally, the classification results have been improved after the intensity data is radiometrically corrected. An improvement of 3.5% for combined three-intensity images and 5.5% for combined three-intensity images with DSM are achieved as shown in Table 3 and Table 4. In particular, the radiometric correction has improved the classification results of hard classes (e.g., buildings, roads, and soil) rather than soft classes (e.g., trees and grass).

Figure 6. Classified images, from combined corrected intensity images (left) and combined corrected intensity images with DSM (right).

Table 3. Confusion matrix of the combined three corrected intensity images

Classified points	**Reference points**							**Total**	**User's**
	U	**Buildings**	**Trees**	**Roads**	**Grass**	**Soil**	**Wetland**	**row**	**Acc. (%)**
U	0	0	0	0	1	0	0	1	
Buildings	0	20	4	6	1	1	0	32	62.50
Trees	0	2	29	0	4	4	0	39	74.36
Roads	0	0	2	13	2	0	0	17	76.47
Grass	0	0	2	2	58	3	0	65	89.23
Soil	0	5	5	2	5	14	0	31	45.16
Wetland	0	1	5	0	3	2	4	15	26.67
Total column	0	28	47	23	74	24	4	200	
Producer's Acc. (%)		71.43	61.70	56.52	78.38	58.33	100.00		

Overall accuracy: 69.00%, overall Kappa statistic: 0.603

Table 4. Confusion matrix of the combined three corrected intensity images with DSM

Classified points	U	Buildings	Trees	Roads	Grass	Soil	Wetland	Total row	User's Acc. (%)
	Reference points								
U	0	0	0	0	0	0	0		
Buildings	0	23	2	0	1	1	0	27	85.19
Trees	0	2	41	0	8	2	0	53	77.36
Roads	0	0	0	18	2	1	0	21	85.71
Grass	0	0	2	2	55	3	0	62	88.71
Soil	0	3	2	3	8	16	1	33	48.48
Wetland	0	0	0	0	0	1	3	4	75.00
Total column	0	28	47	23	74	24	4	200	
Producer's Acc. (%)		82.14	87.23	78.26	74.32	66.67	75.00		

Overall accuracy: 78.00%, overall Kappa statistic: 0.715

5. CONCLUSIONS

This paper investigates the potential use of the newly developed multispectral LiDAR sensor for land cover classification in urban areas. The summary of the overall classification accuracies of the tested data is shown in Figure 7. The achieved results indicate that multispectral LiDAR data can be used efficiently in land cover classification rather than the single-wave LiDAR data. The investigation also indicated that the elevation data should be combined with the intensity data to improve the classification accuracy. Moreover, the achieved results have proven that the radiometric correction should be applied to the intensity data to maximize its benefits in land cover classification. Further investigations are underway to explore the capability of multispectral LiDAR data in different applications.

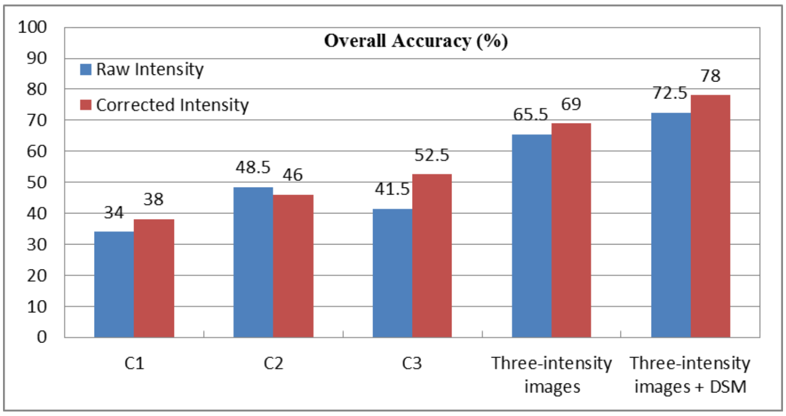

Figure 7. Summary of the overall classification accuracies for the tested data

ACKNOWLEDGMENT

This research work is supported by the Discovery Grant from the Natural Sciences and Engineering Research Council of Canada (NSERC) and the Ontario Trillium Scholarship (OTS). The authors would like to thank Dr. Paul E. LaRocque from Teledyne Optech for providing the LiDAR data from the world's first commercial multispectral airborne LiDAR system, the Optech Titan.

REFERENCES

Briese, C., Pfennigbauer, M., Lehner, H., Ullrich, A., Wagner, W. and Pfeifer, N., 2012. Radiometric calibration of multi-wavelength airborne laser scanning data. ISPRS Ann. Photogramm. Remote Sens. Spat. Inf. Sci, 1, pp.335-340.

Danson, F.M., Gaulton, R., Armitage, R.P., Disney, M., Gunawan, O., Lewis, P., Pearson, G. and Ramirez, A.F., 2014. Developing a dual-wavelength full-waveform terrestrial laser scanner to characterize forest canopy structure. Agricultural and Forest Meteorology, 198, pp.7-14.

Douglas, E.S., Martel, J., Li, Z., Howe, G., Hewawasam, K., Marshall, R.A., Schaaf, C.L., Cook, T.A., Newnham, G.J., Strahler, A. and Chakrabarti, S., 2015. Finding leaves in the forest: the dual-wavelength Echidna lidar. IEEE Geoscience and Remote Sensing Letters, 12(4), pp.776-780.

Morsy, S., Shaker, A., El-Rabbany, A. and LaRocque, P.E., 2016. Airborne multispectral LiDAR data for land-cover classification and land/water mapping using different spectral indexes. ISPRS Annals of Photogrammetry, Remote Sensing and Spatial Information Sciences, pp.217-224.

Shi, S., Song, S., Gong, W., Du, L., Zhu, B. and Huang, X., 2015. Improving backscatter intensity calibration for multispectral lidar. IEEE Geoscience and Remote Sensing Letters, 12(7), pp.1421-1425.

Titan Brochure and Specifications, 2015. Optech Titan Multispectral Lidar System - High Precision Environmental Mapping, Retrieved August 17, 2016, from http://www.teledyneoptech.com/wp-content/uploads /Titan-Specsheet-150515-WEB.pdf.

Wallace, A., Nichol, C. and Woodhouse, I., 2012. Recovery of forest canopy parameters by inversion of multispectral LiDAR data. Remote Sensing, 4(2), pp.509-531.

Wang, C.K., Tseng, Y.H. and Chu, H.J., 2014. Airborne dual-wavelength lidar data for classifying land cover. Remote Sensing, 6(1), pp.700-715.

Wei, G., Shalei, S., Bo, Z., Shuo, S., Faquan, L. and Xuewu, C., 2012. Multi-wavelength canopy LiDAR for remote sensing of vegetation: Design and system performance. ISPRS journal of photogrammetry and remote sensing, 69, pp.1-9.

Wichmann, V., Bremer, M., Lindenberger, J., Rutzinger, M., Georges, C. and Petrini-Monteferri, F., 2015. Evaluating the potential of multispectral airborne LiDAR for topographic mapping and land cover classification. ISPRS Annals of the Photogrammetry, Remote Sensing and Spatial Information Sciences, 1, pp.113-119.

Woodhouse, I.H., Nichol, C., Sinclair, P., Jack, J., Morsdorf, F., Malthus, T.J. and Patenaude, G., 2011. A multispectral canopy LiDAR demonstrator project. IEEE Geoscience and Remote Sensing Letters, 8(5), pp.839-843.

Yan, W.Y. and Shaker, A., 2014. Radiometric correction and normalization of airborne LiDAR intensity data for improving land-cover classification. IEEE Transactions on Geoscience and Remote Sensing, 52(12), pp.7658-7673.

Yan, W.Y., Shaker, A. and El-Ashmawy, N., 2015. Urban land cover classification using airborne LiDAR data: A review. Remote Sensing of Environment, 158, pp.295-310.

Yan, W.Y., Shaker, A., Habib, A. and Kersting, A.P., 2012. Improving classification accuracy of airborne LiDAR intensity data by geometric calibration and radiometric correction. ISPRS journal of photogrammetry and remote sensing, 67, pp.35-44.